GEOPHYSICS, VOL. 83, NO. 3 (MAY-JUNE 2018); P. B119–B132, 25 FIGS., 1 TABLE.
10.1190/GEO2017-0319.1

Case History

Rock-physics characterization of bitumen carbonates: A case study

Hemin Yuan[1], De-Hua Han[2], Luanxiao Zhao[3], Qi Huang[2], and Weimin Zhang[4]

ABSTRACT

Bitumen carbonate is an important source of bitumen, and knowledge of its properties needs to be improved. Owing to its high viscosity, most production methods of bitumen involve thermal techniques. Bitumen properties change tremendously during thermal production, which can inevitably affect the properties of bitumen carbonates. Moreover, the high pressure applied for steam injection can also impact the properties of bitumen carbonates. The variations of reservoir properties are indicators of a steam-affected zone, and thus they are significant for reservoir monitoring. To reveal the responses of bitumen carbonates under different pressure and temperature conditions, two bitumen carbonate samples are measured in the laboratory. We first develop a method that enables the estimation of porosity and bitumen saturation simultaneously. Then, the samples are exposed to various differential pressures, covering the in situ effective pressure range, to study the influence of pressure on velocities. Afterward, different temperatures are used to test the temperature sensitivity of the two samples. A histogram analysis of the velocity variations is also conducted to investigate the effects of distinct porosity and bitumen saturation. After washing off the bitumen, the clean samples are also measured and compared with the as-is samples, so as to check the impacts of bitumen on the carbonate samples. We have determined that porosity, bitumen saturation, pressure, and temperature can all have a noticeable influence on the velocities of bitumen carbonates. Although the research is in its initial stage, it can help improve our understanding of bitumen carbonates and also assist in monitoring the steam-affected zone during thermal production.

INTRODUCTION

Because conventional oil and gas reservoirs are depleting nowadays, an increasing number of studies pay attention to unconventional reservoirs. As one kind of unconventional reservoir, bitumen is becoming increasingly important because of its enormous supply all over the world. The amount of bitumen, plus heavy oil and extra heavy oil, is double the resource of conventional hydrocarbon resources, and even bitumen itself has a similar amount as conventional oil and gas reservoirs (Meyer and Attanasi, 2003; Alboudwarej et al., 2006). Bitumen represents approximately 30% of the world total hydrocarbon reservoir, close to the amount of conventional oil. Of this significant amount of bitumen, approximately 69% is distributed in bitumen sands, whereas the remaining 31% is distributed in bitumen carbonates (Priaro, 2014), suggesting that bitumen sands and bitumen carbonates are important hosts of sources.

Bitumen has extremely high viscosity. The viscosity is usually greater than 10 Pa · s, and could even be as high as 1000 Pa · s for extra heavy bitumen. Moreover, the viscosity is temperature dependent, and it decreases quickly with increasing temperature. Schmitt (2002, 2004) studies the viscosity of bitumen and plots the illustrative relation between viscosity and temperature as shown in Figure 1. It reveals that the bitumen viscosity drops over five magnitudes as temperature increases from 0°C to 200°C, indicating its high sensitivity to temperature. These special properties of bitumen inevitably affect the properties of bitumen-saturated sands and carbonates.

Manuscript received by the Editor 16 May 2017; revised manuscript received 22 January 2018; published ahead of production 14 February 2018; published online 09 April 2018.
[1]University of Copenhagen, Department of Geosciences and Natural Resource Management, Copenhagen, Denmark. E-mail: hya@ign.ku.dk.
[2]University of Houston, Department of Earth and Atmospheric Sciences, Houston, Texas, USA. E-mail: dhan@central.uh.edu; huangqiron@yahoo.com.
[3]Tongji University, State Key Laboratory of Marine Geology, Shanghai, China. E-mail: zhaoluanxiao@tongji.edu.cn.
[4]Cenovus Energy Inc., Calgary, Canada. E-mail: weimin.zhang@cenovus.com.

Batzle et al. (2006) study the seismic properties of bitumen, whereas Han et al. (2006, 2008) measure the S-wave velocities and study the acoustic properties of bitumen sands. The variation of bitumen sand properties with temperature and pressure is also detailed by Li et al. (2016b). Others also did measurements and research on bitumen sand samples (Rojas et al., 2008; Kato, 2010; Wolf, 2010; Yuan et al., 2015). Different from bitumen sands, bitumen carbonates are generally stiffer rocks with smaller porosity and lower permeability. Rabbani et al. (2014, 2017) measure the bitumen-saturated Grosmont carbonates under different pressure and temperature conditions and try to simulate the carbonate samples with geometric models. Chen et al. (2015) extend Rabbani's measurements to a broader pressure range. Yuan et al. (2017) compare the bitumen carbonates and bitumen sands in various aspects. However, little research has been conducted on bitumen carbonates systematically, including the effects of pressure and temperature on velocity, as well as the porosity and saturation.

According to the special properties of bitumen and bitumen carbonate, we develop a method to estimate the porosity and bitumen saturation. The method involves using the Archimedes law method to measure the bulk volume of the sample and using a porosimeter to estimate the volume of empty pore space in sample. Afterward, the velocities of the bitumen carbonates at various pressure and temperature conditions are measured, and the differences between them are compared and analyzed. The peculiar trend of the bitumen carbonates under temperature measurement is also elaborated by combining the properties of bitumen. Then, the bitumen in samples is washed away, and the comparisons between the clean samples and as-is samples are also performed to inspect the influence of bitumen on carbonate samples. The scanning electron micrographs (SEMs) and thin section imaging are also conducted on the clean samples to investigate the pore size and distribution.

POROSITY AND SATURATION MEASUREMENT

Porosity is an elementary property of rocks, which is the basis for further analysis and modeling. The Archimedes law method is a commonly used method for porosity estimation. Sharma and Prasad (2009) apply the Archimedes law method on carbonates. Dirgantara et al. (2011) use the Archimedes law method for estimating the porosity of coals. Using the Archimedes law method on porosity estimation of mudrocks is also documented by Kuila (2013). Porosity estimation of heavy oil sand samples using the Archimedes law method was introduced by Li et al. (2016a). However, conventional porosity measurement methods either have large errors or cannot measure the true porosity, especially for partially saturated samples. Archimedes law states that when a solid body is submerged in a liquid, the liquid exerts an upward buoyant force on the body that is equal to the weight of the displaced fluid. It measures the volume increase of water after a sample is immersed, and thus it can be used to determine the bulk volume of the rock sample. However, to estimate porosity, it requires that the sample is fully water saturated or oil saturated, whereas the true samples are usually not fully saturated with part of empty pore space. Thus, the assumption of full saturation can lead to underestimation of bulk density and overestimation of true porosity. The porosimeter method is based on Boyle's law, which states that the product of volume and pressure is constant when temperature is stable. It can provide relatively accurate prediction of the empty pore space. However, as explained above, pore space of true sample is usually partially saturated, and thus the porosimeter method can only measure apparent porosity that is smaller than true porosity.

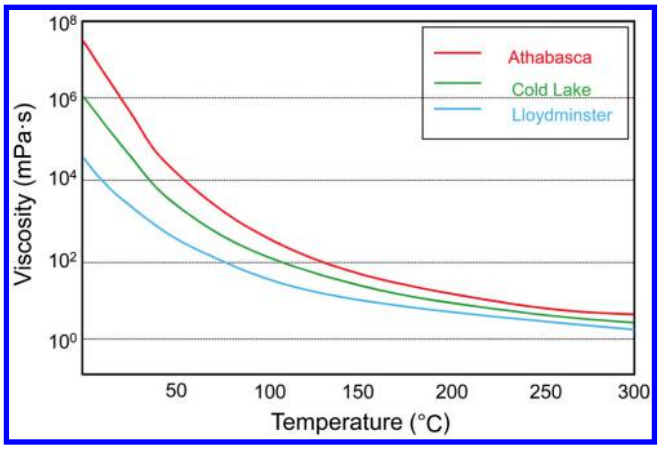

Figure 1. The bitumen viscosity under different temperatures (Schmitt, 2004). The red line represents the viscosity of bitumen in Athabasca, the green line represents the viscosity of bitumen in Cold Lake, and the cyan line represents the viscosity of bitumen in Lloydminster.

Considering that bitumen has very high viscosity and cannot flow at room conditions, we develop a method combining the Archimedes law method and the porosimeter method. The Archimedes law method is used for bulk volume measurement and the porosimeter method can estimate the volume of empty pore space. Because the American Petroleum Institute (API) gravity (Ruh et al., 1959) of bitumen is 6.5 (W. Zhang, personal communication, 2014), the true density of bitumen can be derived.

Then, the porosity can be estimated through the steps below:

1) Put the sample into a vacuum drier to remove the water in the pore space. Then, its pore space is only filled with solid bitumen and air.
2) Measure the dry sample weight m_a. This is the weight of the as-is sample that is composed of the carbonate frame and bitumen in the pore space.
3) Measure the sample bulk volume by the Archimedes law method. First, immerse the sample completely in water, measure the weight increase of water m_i. Then, take the sample out and wipe off the water on surface and measure the sample weight m_a'. The sample bulk volume V_b can be estimated by dividing the water weight increase by water density ρ_w.
4) Use a porosimeter to measure the empty pore space V_e (the pore space filled with air). The porosimeter can measure the pore space by changing pressure because the product of pressure and volume is constant when temperature is stable.
5) Calculate the porosity and bitumen saturation.

In step 3, it is possible that the sample imbibes water into the pore space, which can lead to underestimation of weight increase of water. The imbibed water weight m_{ib} is

$$m_{ib} = m_a' - m_a. \tag{1}$$

And the true increase of water weight m_i' is

$$m_i' = m_i + m_{ib} = m_i + (m_a' - m_a). \tag{2}$$

Then, the bulk volume of the sample $V_b = m_i'/\rho_w$, and the bulk density of the dry sample $\rho_b = m_a/V_b$ can be calculated.

Because the dry sample is composed of frame, bitumen, and air in pore space, the sample bulk density can be represented as

$$\rho_b = \rho_m(1-\phi) + \rho_o\phi S_o + \rho_a\phi(1-S_o), \tag{3}$$

where ρ_m is the mineral density, ρ_o is the bitumen density, ρ_a is the air density, ϕ is the true porosity, and S_o is the bitumen saturation. Considering that air density is 0.0012 g/cm^3 at room conditions, which is negligible, equation 3 can be simplified to

$$\rho_b = \rho_m(1-\phi) + \rho_o\phi S_o. \tag{4}$$

In step 4, the empty pore space V_e can be obtained from the porosimeter, while it can also be denoted as the pore space unfilled with bitumen

$$V_e = V_b\phi(1-S_o). \tag{5}$$

The mineral density ρ_m is 2.71 g/cm^3 for calcite, which is also verified by grain density measurement of the clean rock (after washing the bitumen). Then, in equations 4 and 5, there are five known parameters ρ_b, ρ_m, ρ_o, V_e, and V_b, and two unknown parameters ϕ and S_o. Thus, the porosity and bitumen saturation can be derived according to

$$\phi = \frac{\rho_m - \rho_o\frac{V_e}{V_b} - \rho_b}{\rho_m - \rho_o}, \tag{6}$$

$$S_o = \frac{\rho_m - \rho_m\frac{V_e}{V_b} - \rho_b}{\rho_m - \rho_o\frac{V_e}{V_b} - \rho_b}. \tag{7}$$

The estimated porosity and saturation of the samples are shown in Table 1.

RESULTS

The measured samples 156A and 156B are from the Grosmont Formation that is located in the Western Canadian Sedimentary Basin, Alberta, Canada. The Grosmont Formation is a stratigraphic unit of Upper Devonian age, primarily composed of carbonate that is uniquely characterized by open fractures and large vugs. It is estimated that more than 318 billion barrels of bitumen resource is assigned to the Grosmont Formation (Bakhorji, 2010). Pictures of the two samples are displayed in Figure 2, and the related information is exhibited in Table 1.

In Figure 2, it can be seen that bitumen is heterogeneously distributed in both samples. Besides, sample 156A has a darker appearance than 156B, suggesting higher bitumen content. In Table 1, despite the similar depth of the two samples, 156A has a smaller porosity but higher bitumen saturation than 156B, consistent with the observations from Figure 2. The bitumen distribution, porosity, and saturation all affect the properties of the bitumen carbonate samples, especially at various pressure and temperature conditions.

Velocity under different pressures

The pressure effect on the properties of bitumen carbonates mainly relies on the opening and closing of the cracks and low-aspect-ratio pores. The cracks can be closed at high pressure, and thus the moduli of the bitumen carbonates increase, and vice versa. However, the carbonate samples exhibit distinctive sensitivity to pressure, which may be related to different porosity, bitumen saturation, and pore structure (Gomez et al., 2007; Scotellaro and Mavko, 2008). To test the pressure sensitivity of the two carbonate samples, they are exposed to a differential pressure from 0 to 3000 psi with an interval of 300 psi, which covers the in situ effective pressure (2100 psi). The measurements are performed under

Table 1. The measured porosities and relative information of the two samples. The depth information is provided by Cenovus Energy Inc., the weight is measured by an electronic scale, the length and diameter are measured by a vernier caliper, the sample length before and after heating and pressuring are measured by a vernier caliper, and the porosity and bitumen saturation are estimated through the developed method.

Sample no.	156A	156B
Depth (m)	579.44	579.44
Weight (g)	48.39	47.60
Diameter (mm)	25.11	25.09
Length before heating and pressuring (mm)	40.50	41.38
Length after heating and pressuring (mm)	40.47	41.37
Time uncertainty of P-wave (μs)	0.3	0.3
Time uncertainty of S-wave (μs)	0.15	0.15
Porosity	15.5%	18.2%
Error of porosity	2.2%	2.1%
Bitumen saturation	52.4%	43.8%
Error of bitumen saturation	8.8%	8.3%

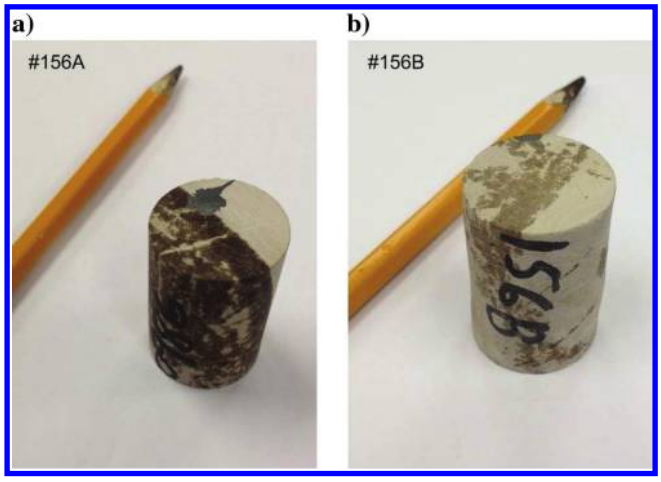

Figure 2. Pictures of the bitumen carbonates (a) 156A and (b) 156B from Alberta, Canada. Sample 156A has a darker appearance than 156B, indicating a higher bitumen content in 156A.

two conditions: an as-is condition and a wet condition. The as-is condition is the measurement conducted without pore-pressure control, which means that part of the pore space is filled with air during measurement process. The wet measurement is executed after water injection, and the sample is fully saturated without air in the pore space. The measured P-wave and S-wave velocities of the two samples are shown in Figures 3 and 4.

In Figures 3 and 4, the P-wave and S-wave velocities of 156A and 156B increase with pressure. Besides, the velocities (V_P and V_S) increase quickly when the pressure is less than 1200 psi, and increase relatively slowly at a high pressure greater than 1200 psi. This is because the cracks are closed more readily at the initial stage, and most cracks are closed as the pressure increases, leading to increasing difficulty to close more cracks and pores. In addition, the wet sample has a larger V_P and smaller V_S than the as-is sample, owing to the water saturation effect. According to the Gassmann equation (Gassmann, 1951), water saturation can effectively increase rock's bulk modulus, whereas it has no contribution to shear modulus. Given the increase of rock density due to water saturation, it is reasonable to expect a larger V_P and smaller V_S, and correspondingly, a higher V_P/V_S ratio of the wet sample.

Moreover, compared with 156B, V_P and V_S of 156A are greater, but they increase less during the pressuring process (V_P increases 3.1% and V_S increases 4.8%, whereas V_P of 156B increases 11.7% and V_S increases 6.6%). The differences are probably related to porosity, bitumen saturation, and pore structure, which are further discussed in the "Discussion" section. The bitumen property and bulk compositions should be similar, considering that the two samples are at the same depth and from the same well. Nevertheless, sample 156A has smaller porosity and higher bitumen saturation. Given that bitumen is in a solid state with a large bulk modulus and shear modulus at room conditions (bulk modulus is 3.01 GPa and shear modulus is 0.13 GPa, as predicted by the Fluids of Applied Geophysics [FLAG] program), it is reasonable to expect the sample with higher bitumen saturation to have larger bulk modulus and shear modulus. For better comparison, the histogram analysis of V_P and V_S variations are performed, as shown in Figure 5a and 5b.

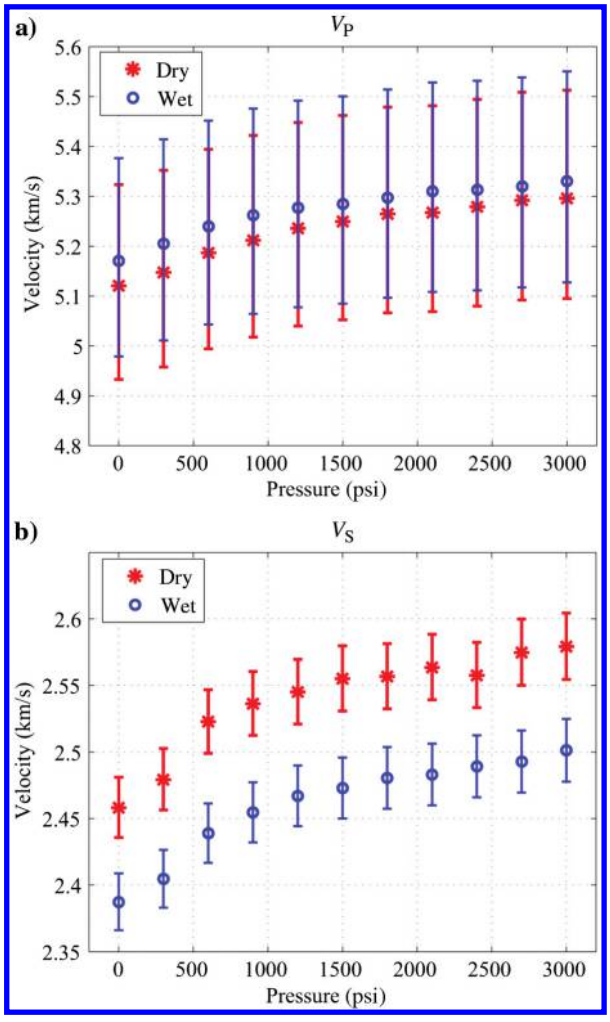

Figure 3. (a) The P-wave velocity and (b) S-wave velocity variations with pressure of sample 156A. The red asterisks represent the velocities of the dry sample; the blue circles represent the velocities of the wet sample that is fully saturated with water. Error bars are also plotted.

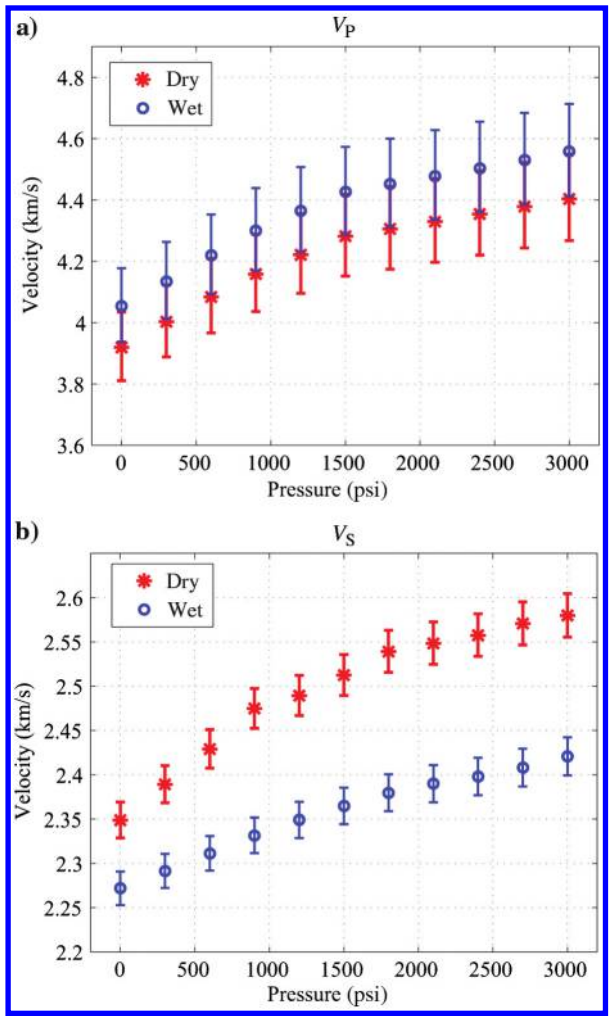

Figure 4. (a) The P-wave velocity and (b) S-wave velocity variations with pressure of sample 156B. The red asterisks represent the velocities of the dry sample; the blue circles represent the velocities of the wet sample that is fully saturated with water. Error bars are also plotted.

In Figure 5, sample 156B has a larger increase of velocity in V_P and V_S, and the corresponding relative rate of increase is also greater, which suggests that 156B is more sensitive to pressure than 156A. It is because the larger porosity and lower bitumen saturation leave more empty space in 156B, making it more compressible. Although the bitumen in the pore space increases the moduli of the rock under room conditions, it can also impede the microcracks from closing and thus mitigate the sensitivity of rock to pressure.

Velocity under different temperatures

Temperature can severely influence the properties of bitumen carbonates by affecting the bitumen viscosity. The viscosity and moduli of bitumen drop drastically with rising temperature, as displayed in Figures 6 and 7, which are also predicted by the FLAG program. The measured velocities at different temperatures (from 10°C to 120°C) of 156A and 156B are displayed in Figures 8 and 9.

In Figure 6, it can be seen that the bitumen viscosity drops dramatically with the rising temperature, and it declines about five magnitudes when the temperature rises from 10°C to 100°C, demonstrating its temperature sensitivity. The bulk and shear moduli also show drastic drop with rising temperature owing to the viscosity. The bulk modulus decreases 45%, and the shear modulus almost reaches zero when the temperature is greater than 60°C. These temperature-dependent properties of viscosity and moduli inevitably affect the elastic properties of bitumen carbonates.

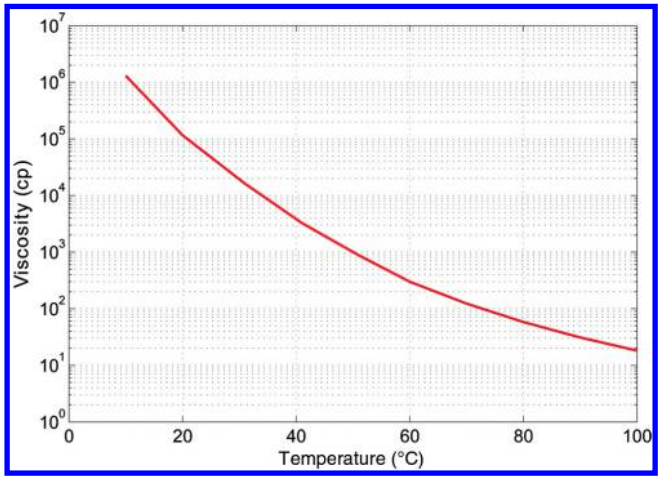

Figure 6. The viscosity of the bitumen versus temperature. The API value of the bitumen is 6.5.

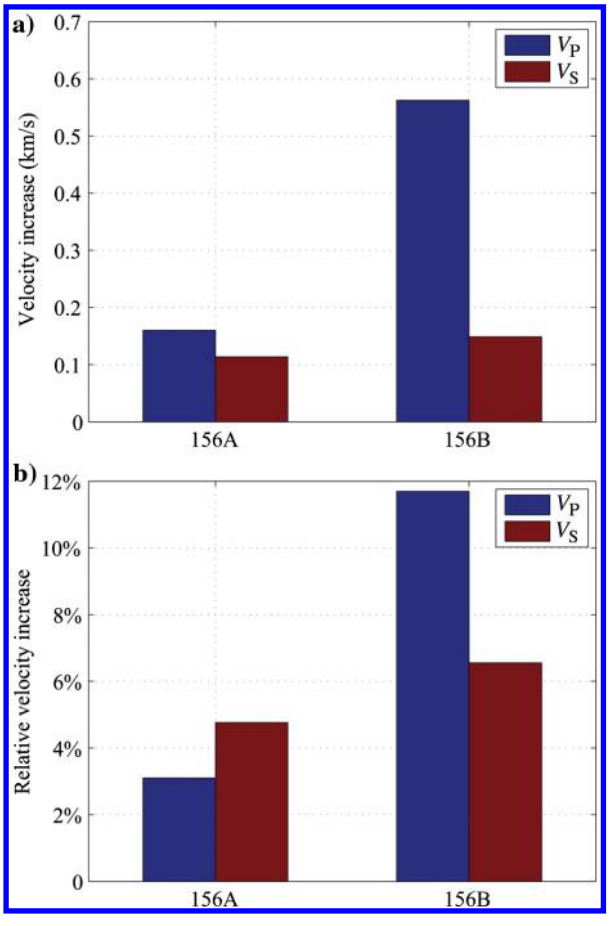

Figure 5. (a) Velocity increase of the samples with pressure increasing from 0 to 3000 psi. (b) Relative velocity increase. The blue bars represent the P-wave velocity, and the red bars represent the S-wave velocity.

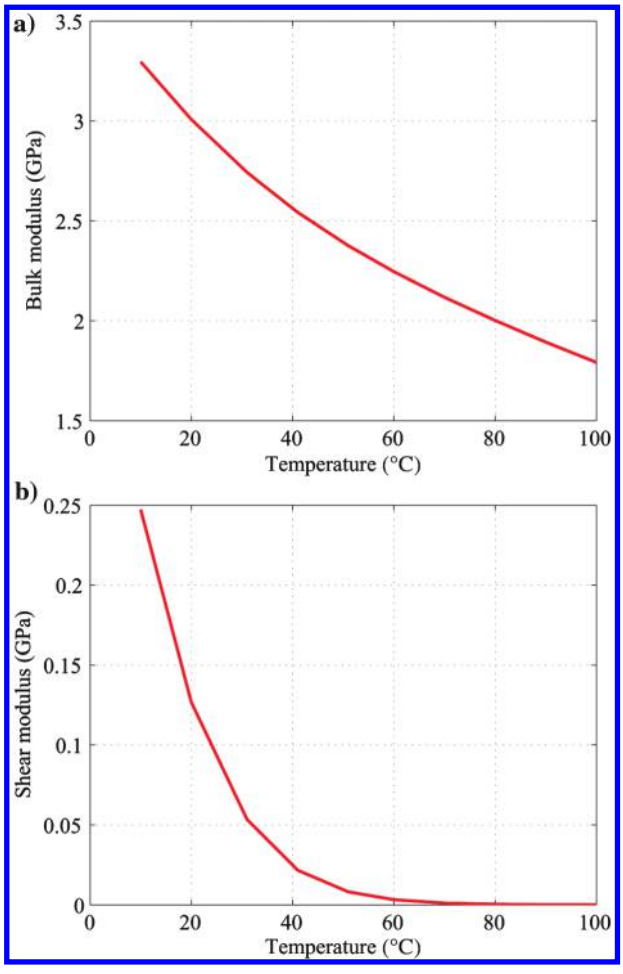

Figure 7. The (a) bulk modulus and (b) shear modulus of the bitumen versus temperature. The bulk modulus and shear modulus decrease drastically with the increasing temperature.

In Figures 8 and 9, V_P of 156A and 156B decreases with rising temperature. Sample 156A has a V_P declining from 5.32 to 4.79 km/s, close to 10% drop; whereas 156B has a V_P declining from 4.41 to 4.06 km/s, approximately 8% drop. Moreover, compared with wet samples, the V_P of dry samples is smaller, which can be explained by the Gassmann theory. The water saturation, although it increases the sample's density, makes a greater contribution to the bulk modulus, resulting in a larger V_P of the wet samples.

The V_S displays a similar trend to V_P, and it also declines with rising temperature. Sample 156B still displays a greater velocity drop than 156A. The V_S of 156A declines from 2.5 to 2.29 km/s, close to 8.4% drop; whereas V_S of 156B declines from 2.3 to 2.11 km/s, approximately 8.2% drop. Besides, the V_S values of wet samples are smaller than those of dry samples because the water saturation makes no contribution to the rock shear modulus, whereas it increases rock density.

Moreover, it is noticeable that when temperature is greater than 60°C, the velocities (V_P and V_S) decrease faster than the velocities at lower temperature. Two potential reasons may be accountable for the phenomenon. The first one is that some air remains in the pore space and it mixes with the bitumen when temperature is high and bitumen is in liquid phase. The mixture of air and liquid bitumen form the iso-stress conditions and thus cause low velocities. The second reason may be related to the water-weakening effect. The injected water softens the carbonate frame, and high temperature can promote the process (Carles and Lapointe, 2004; Korsnes et al., 2008), and hence lead to a quick velocity drop at high temperature.

To better compare the temperature sensitivity of the two samples, the histogram velocity variations of the two samples are calculated and displayed in Figure 10a and 10b. It can be seen that 156A has greater changes of velocity than 156B during heating process, suggesting that 156A is more sensitive to temperature, which is because the higher bitumen content in 156A makes it more susceptible to bitumen properties. Because bitumen moduli drop dramatically with rising temperature, the high bitumen saturation can cause more velocity drop of 156A.

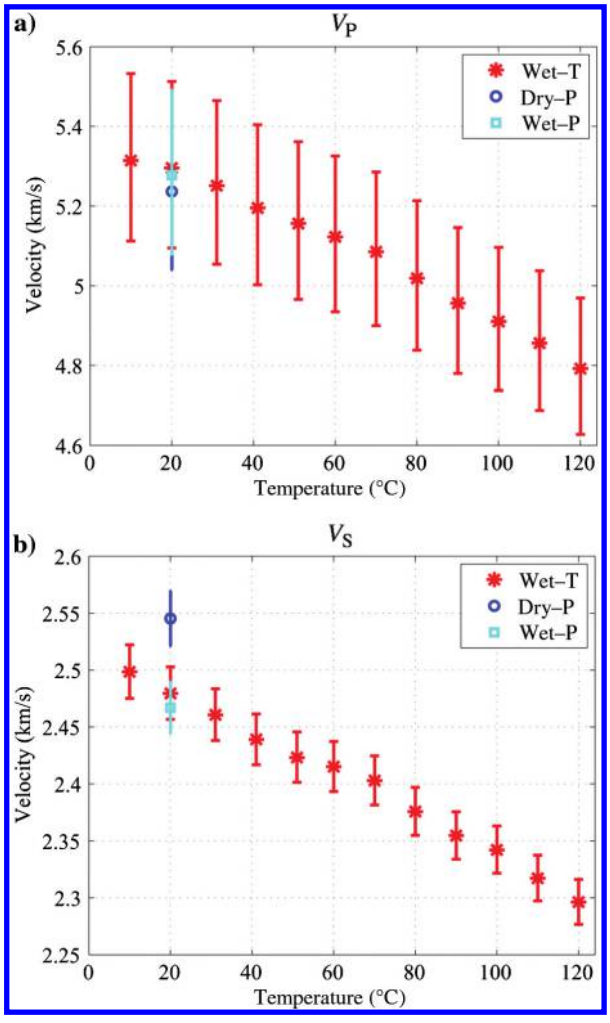

Figure 8. (a) The P-wave velocity and (b) S-wave velocity variations with temperature of sample 156A. The red asterisks represent the velocity of the wet sample during the heating process, the blue circles represent the velocity of the dry sample during the pressuring process, and the cyan squares represent the velocity of the wet sample measured during the pressuring process. Error bars are also plotted.

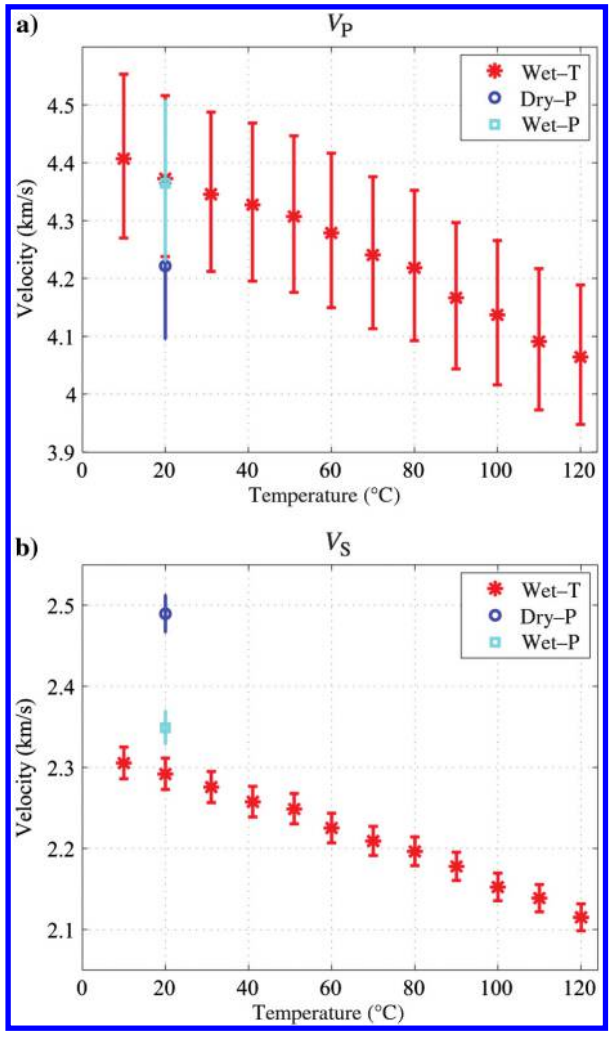

Figure 9. (a) The P-wave velocity and (b) S-wave velocity variations with temperature of sample 156B. The red asterisks represent the velocity of the wet sample during the heating process, the blue circles represent the velocity of the dry sample during the pressuring process, and the cyan squares represent the velocity of the wet sample measured during the pressuring process. Error bars are also plotted.

In addition, compared with the velocity variation with pressure, the velocities of 156A appear to be more sensitive to temperature than pressure at laboratory measurement conditions. The V_P declines approximately 10% and V_S declines approximately 8.4% with temperature from 10°C to 120°C, whereas V_P drops close to 3% and V_P drops to less than 5% with pressure from 3000 to 0 psi. On the other side, the V_P of 156B appears to be more sensitive to pressure than temperature. The V_P drops to less than 8% within the temperature measurement range, whereas it decreases close to 11% within the pressure range. These are also caused by the distinctive porosity and bitumen saturation of the two samples. The large porosity and low bitumen saturation of 156B render it more susceptible to pressure variation, whereas the low porosity and high bitumen saturation of 156A cause it to be more easily affected by temperature.

To confirm that the velocity variation is mainly caused by bitumen viscosity change rather than the frame damage due to bitumen expansion, we also conduct two measurements of the samples, as displayed in Figure 11. The first measurement is performed before the samples are heated, and thus it can reflect the properties of the original state, whereas the second measurement is performed after the heating cycle (the sample is heated at 120°C and then cooled to 20°C). It is clear that there is no significant difference between the two measurements, which suggests that the heating cycle does not cause noticeable changes to the rock frame.

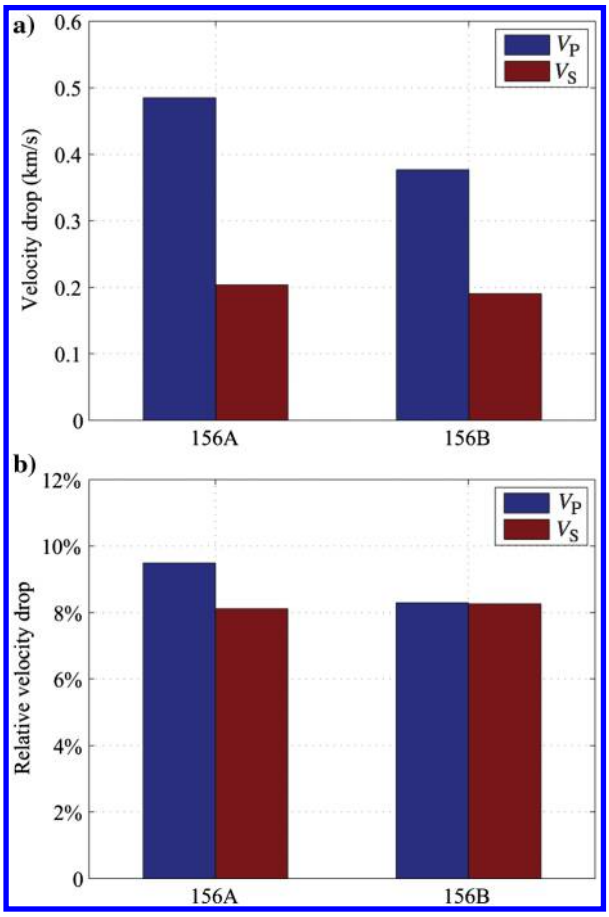

Figure 10. (a) Velocity drop of the samples with temperature increasing from 10°C to 120°C. (b) Relative velocity drop. The blue bars represent the P-wave velocity, and the red bars represent the S-wave velocity.

Clean sample versus as-is sample

The above measurements and analysis are for as-is samples that are partially saturated with bitumen. To make the analysis more convincing, it is necessary to compare the properties of the carbonate samples with and without bitumen. Hence, the two samples are cleaned to directly investigate the properties of clean carbonate samples. The cleaned samples are shown in Figure 12, which display a much lighter appearance than the original samples in Figure 2. The energy-dispersive X-ray spectroscopy (EDS) analysis in Figure 12c also demonstrates that the mineral is mainly calcite.

With cleaned samples, SEM and thin-section imaging can be applied to investigate the pore size and distribution, and the results are shown in Figures 13 and 14. It is clear in Figures 13a and 14a that

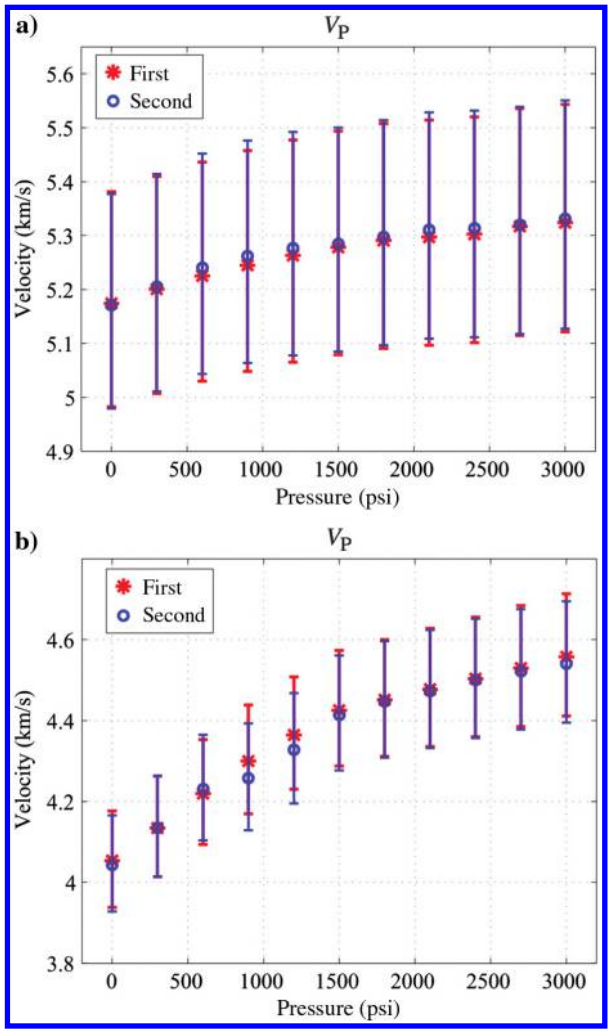

Figure 11. Velocity measurement of the samples before and after the heating process of (a) 156A and (b) 156B. The red asterisks represent the first measurement before the sample is heated, and the blue circles represent the second measurement after the sample is heated (and cooled). The two measurements are performed at 20°C. The two measurements do not show significant changes, suggesting that there are no noticeable changes on the two samples caused by heating. Error bars are also plotted.

pores are well-developed with good connectivity in both samples. In the thin sections (Figures 13b, 13c, 14b, and 14c), it can be seen that the pores are relatively homogeneously distributed and most of them are connected. Besides, the intergranular pores are irregularly shaped, making it difficult to determine the pore aspect ratios. Overall, most of the pores are clean, whereas some bitumen attaches to the grain contact and may remain after cleaning. The remaining bitumen may be one of the factors that can affect the velocities of the clean samples. The 2D porosity is also obtained by applying ImageJ software on the thin sections. The obtained porosities are 14.6% for sample 156A and 16.5% for sample B, respectively, which are close to the measurement results, suggesting the reliability of the method.

For better comparison, the measuring conditions are kept consistent with those for the as-is samples. Figures 15 and 16 display the pressure effect and the corresponding prediction result of Gassmann equation on clean sample 156A, while Figures 17 and 18 display the pressure effect and the corresponding prediction result of Gassmann equation on clean sample 156B. The Gassmann equation is applicable considering the good pore connectivity.

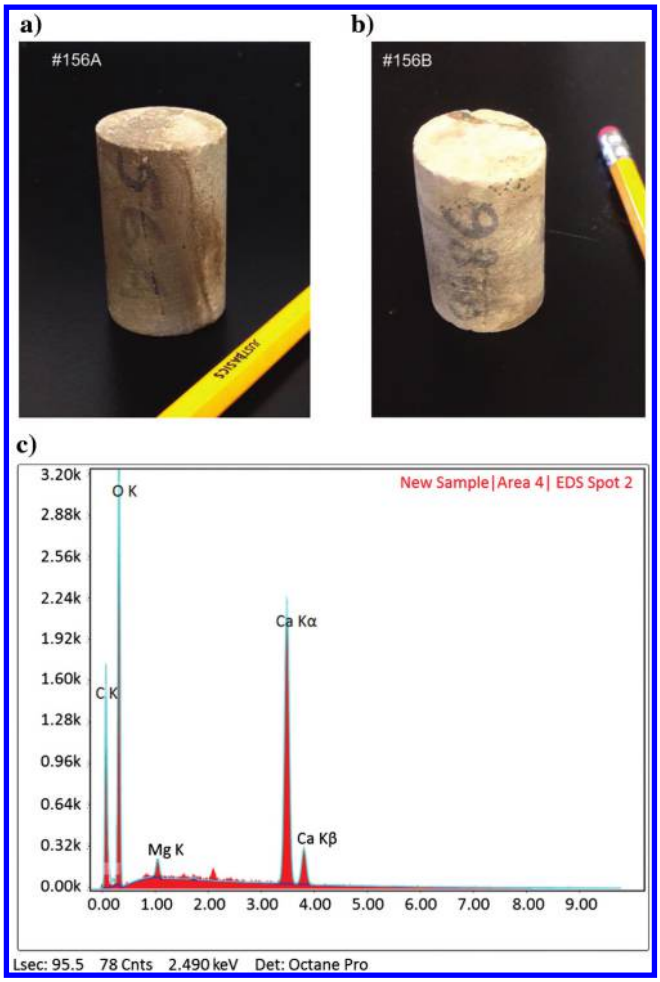

Figure 12. (a) Sample 156A after cleaning the bitumen. (b) Sample 156B after cleaning the bitumen. (c) The EDS analysis of the carbonate. Compared with the original carbonate samples in Figure 2, these two samples display a much lighter appearance due to the fact that the bitumen is eliminated. In the EDS, the rock contains abundant calcium (Ca), but little magnesium (Mg), suggesting that the mineral is mainly calcite, not dolomite.

In Figure 17, it can be seen that for 156B, the wet sample has a larger V_P and smaller V_S than the dry samples, due to water saturation increasing the bulk modulus and density of the rock, whereas

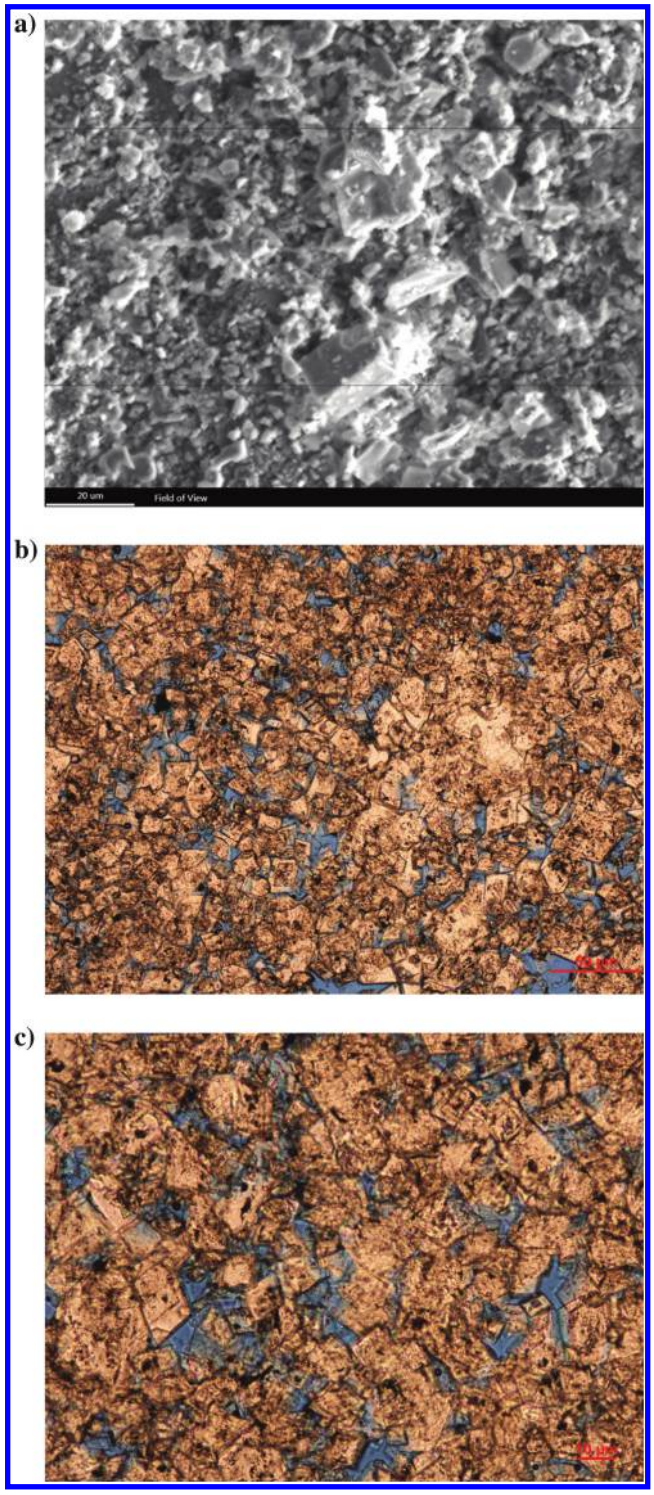

Figure 13. (a) The SEM of sample 156A. (b) Thin section image at 50 μm and (c) thin section image at 10 μm of sample 156A. The scale of the SEM is 20 μm. In the thin sections, the brown color represents the grains, the blue color represents the pore space, and the sporadic black dots represent the remaining bitumen.

the casting has no influence on the shear modulus. Nevertheless, the V_P of the dry 156A sample is larger than the wet sample in Figure 15, which may be due to the porosity and pore structure (e.g., stiff pores with large pore aspect ratio) causing a small increase of bulk modulus that cannot exceed the density increase, resulting in a smaller V_P than the dry sample, consistent with the Gassmann prediction results in Figure 16. It can be seen that the Gassmann equation predicts smaller V_P and V_S of the wet sample. Although the prediction results cannot exactly match the measured data, which may be related to multiple factors such as pore structures, water weakening, frequency, and modulus dispersion (Adam et al., 2006; Adam and Batzle, 2008), the trend does reflect the relative relationship between the velocities of the dry and wet samples. Besides, the relationship of the velocities of the dry and wet 156B sample also coincides with the Gassmann prediction results.

The histogram analysis of velocity variations of the two clean samples is also performed and displayed in Figure 19. For the clean 156A sample, V_P decreases from 5.22 to 5.07 km/s, which is close to a 3% drop; whereas V_S decreases from 2.5 to 2.39 km/s, approximately 4.4% drop. On the other hand, the V_P of the clean 156B sample declines from 4.75 to 4.22 km/s, approximately 11% drop;

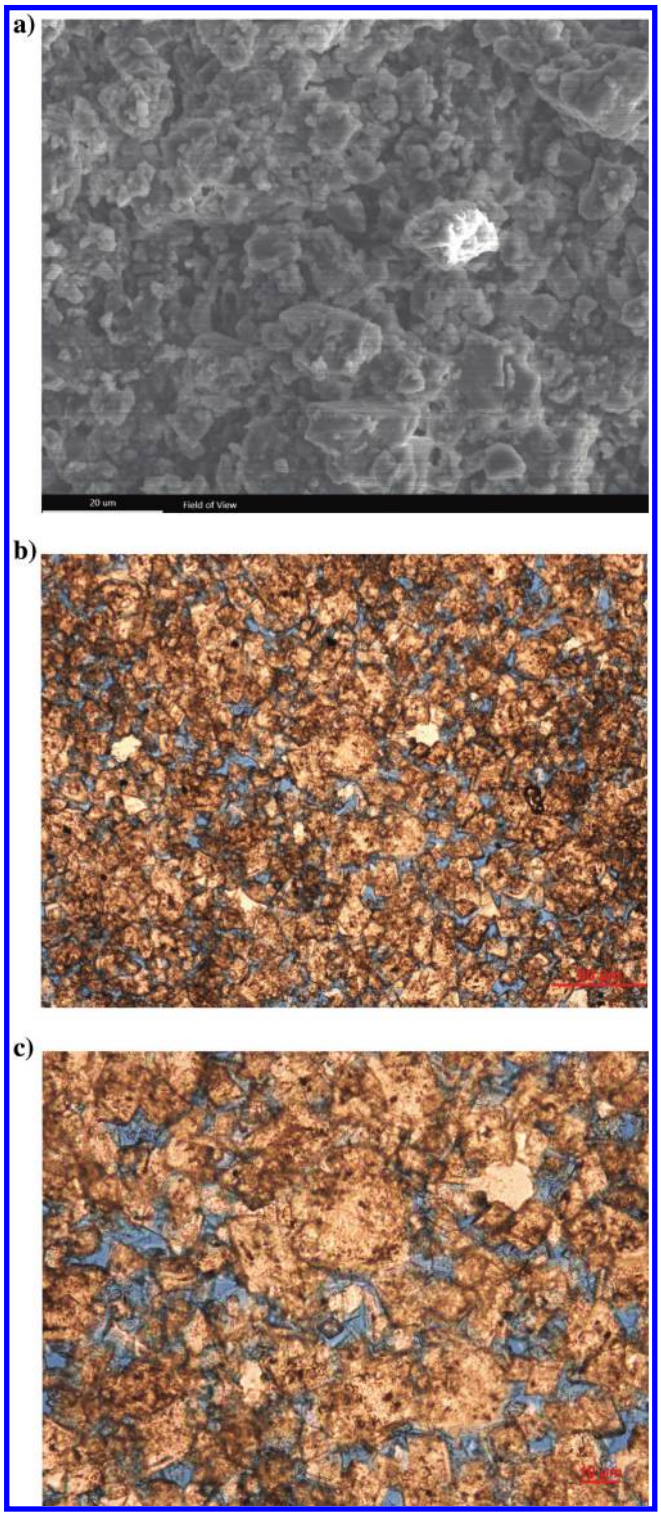

Figure 14. (a) The SEM of sample 156B. (b) Thin section image at 50 μm and (c) thin section image at 10 μm of sample 156B. The scale of the SEM is 20 μm. In the thin sections, the brown color represents the grains, the blue color represents the pore space, and the sporadic black dots represent the remaining bitumen.

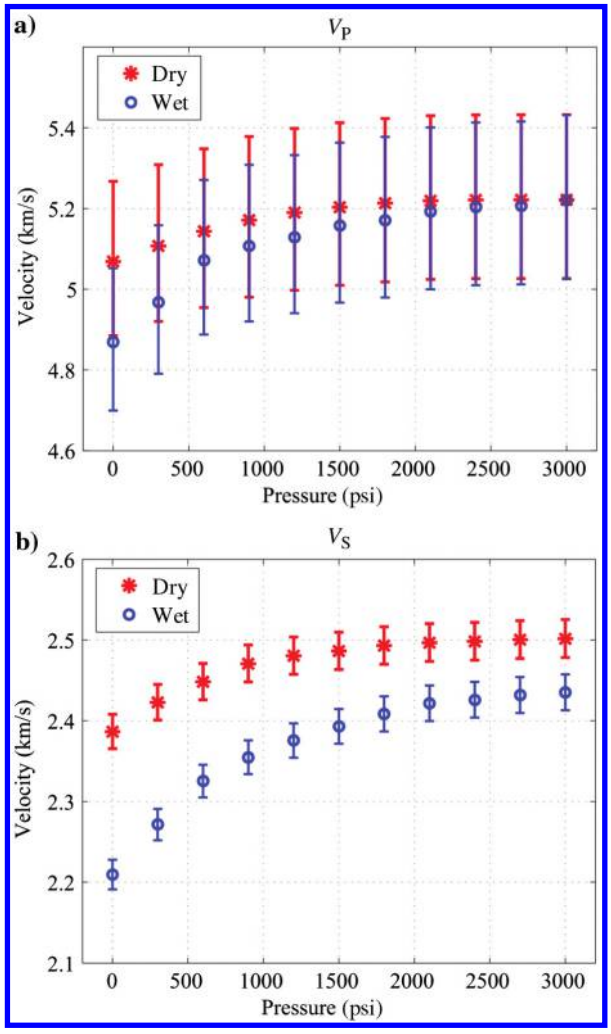

Figure 15. (a) The P-wave velocity and (b) S-wave velocity variations with pressure of cleaned sample 156A. The red asterisks represent the velocities of the dry sample, and the blue circles represent the velocities of the wet sample that is fully saturated with water. Error bars are also plotted.

whereas V_S declines from 2.52 to 2.34 km/s, almost 7.1% drop. Again, 156B appears to be more sensitive to pressure than 156A.

The clean samples are also measured under different temperatures, as displayed in Figures 20 and 21. It can be seen that although the carbonate samples are cleaned, the velocities (V_P and V_S) still decrease with the rising temperature, which we conclude is related to the remaining bitumen in pore space. As shown in Figures 13 and 14, some bitumen remains in pore space even after the cleaning process, which can cause temperature-dependent velocities.

The comparisons of the as-is sample (partially saturated with bitumen) and clean sample are also performed to further investigate the influence of bitumen on the properties of the carbonates, which are displayed in Figures 22, 23, 24, and 25. In Figure 22, it can be found that for 156A, the partially saturated sample has a little larger moduli than the clean sample, owing to the effect of bitumen. The solid bitumen at room conditions can support the carbonate frame, making it relatively stiffer. However, the moduli of the partially saturated sample are temperature dependent. In Figure 23, bulk modulus of the as-is sample is larger than the clean sample at low temperature (less than 60°C), but it declines faster with rising temperature and becomes smaller than the clean sample at high temperature (greater than 80°C), which is also related to the bitumen viscosity variation at different temperatures. At low temperatures, bitumen is in a solid state with large moduli and high viscosity, making the carbonate stiffer. Nevertheless, the bitumen viscosity declines dramatically with rising temperature and it progressively turns to liquid phase, which can expand and may reduce the carbonate moduli. Consequently, the bulk modulus of the as-is sample is below that of the clean sample at higher temperature. On the other hand, the shear modulus does not show noticeable changes between the as-is sample and clean sample, suggesting that bitumen saturation at different temperature causes negligible impact on the shear modulus of the carbonate.

For sample 156B in Figures 24 and 25, the moduli at different temperatures display a similar trend as 156A: the bulk modulus of the as-is sample is larger at a low temperature and smaller at a high temperature. However, it is distinct that the clean sample has a larger bulk modulus than the as-is sample under pressure measurement, which may be related to the pore structure and bitumen saturation, but the mechanism is still unknown, which needs more work in the future.

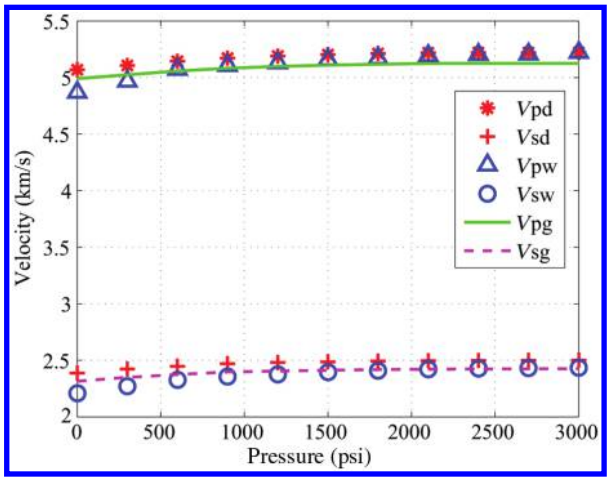

Figure 16. The Gassmann prediction results of sample 156A. The red asterisks represent the V_P of the dry sample, the red plus signs represent the V_S of the dry sample, the blue triangles represent the V_P of the wet sample that is fully saturated with water, the blue circles represent the V_S of the wet sample, the green line represents the predicted V_P with the Gassmann equation, and the magenta dashed line represents the predicted V_P with the Gassmann equation.

Uncertainty analysis

The uncertainty of the porosity estimation comes from the uncertainties of the weight and volume measurements, specifically, the dry sample weight m_a, the sample bulk volume V_b, and volume of the empty pore space V_e. The sample weight is measured through electronic scale with an error range of 0.005 g. The bulk volume is measured through the Archimedes law method, and thus it is essentially measured through weight, which shares the same error range of the electronic scale. In step 3, there may be some uncertainties of water loss during the process of wiping off the water on the sample surface. We assume that the maximum water loss is 0.3 ml, which is a large estimation and the true loss should

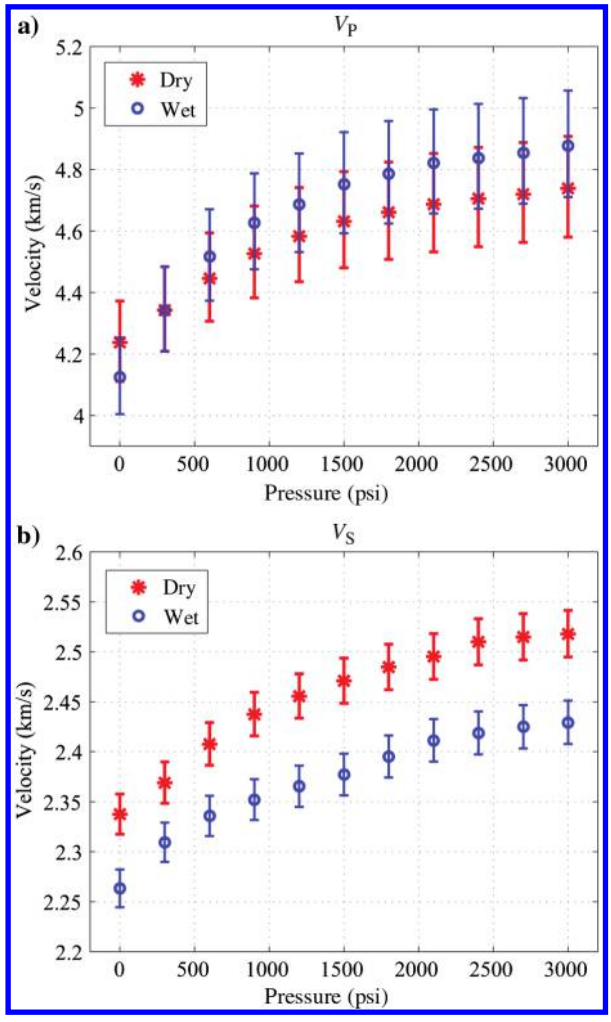

Figure 17. (a) The P-wave velocity and (b) S-wave velocity variations with pressure of the cleaned sample 156B. The red asterisks represent the velocities of the dry sample and the blue circles represent the velocities of the wet sample that is fully saturated with water. Error bars are also plotted.

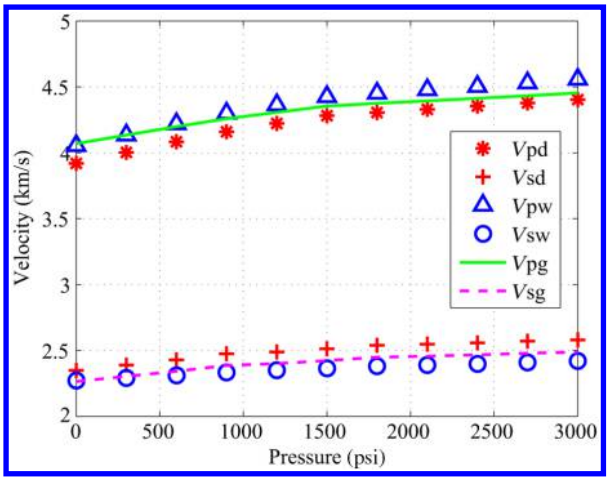

Figure 18. The Gassmann prediction results of sample 156B. The red asterisks represent the V_P of the dry sample, the red plus signs represent the V_S of the dry sample, the blue triangles represent the V_P of the wet sample that is fully saturated with water, the blue circles represent the V_S of the wet sample, the green line represents the predicted V_P with the Gassmann equation, and the magenta dashed line represents the predicted V_S with the Gassmann equation.

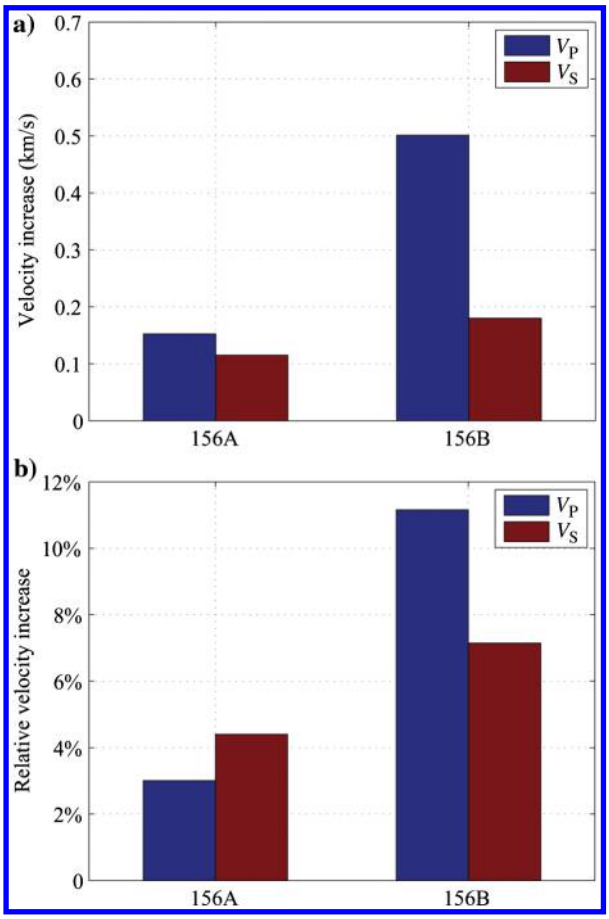

Figure 19. (a) Velocity increase of the clean samples with pressure increasing from 0 to 3000 psi. (b) Relative velocity increase. The blue bars represent the P-wave velocity and the red bars represent the S-wave velocity.

be within the range. The volume of the empty pore space is measured through the porosimeter. The porosimeter measures the pressure with resolution of 0.01 psi, and the corresponding error of empty pore volume is 0.0003%. Then, the uncertainties of porosity can be estimated by introducing the errors of m_a, V_b, and V_e into equations 6 and 7, which are displayed in Table 1.

The uncertainties of the velocity measurement arise from the variations of sample length and the uncertainty of arrival time. The sample lengths are supposed to be constant during the measurements, whereas they may have some variations during the pressuring and heating process. Thus, the sample lengths before and after heating are measured (the error of Vernier caliper, 0.005 mm, is also considered), which are shown in Table 1. Besides, there may be some uncertainties in picking the arrival time. In these measurements, the maximum error of the picked arrival time is assumed to be one-eighth of the signal period, which is actually a very large error and the true error should be within the range. The time errors of 156A and 156B are also displayed in Table 1. With the uncertainties of sample length and the arrival time, the uncertainties of velocities can be estimated, which are also displayed along with measured velocities in Figures 3, 4, 8, 9, 11, 15, 17, 20, and 21.

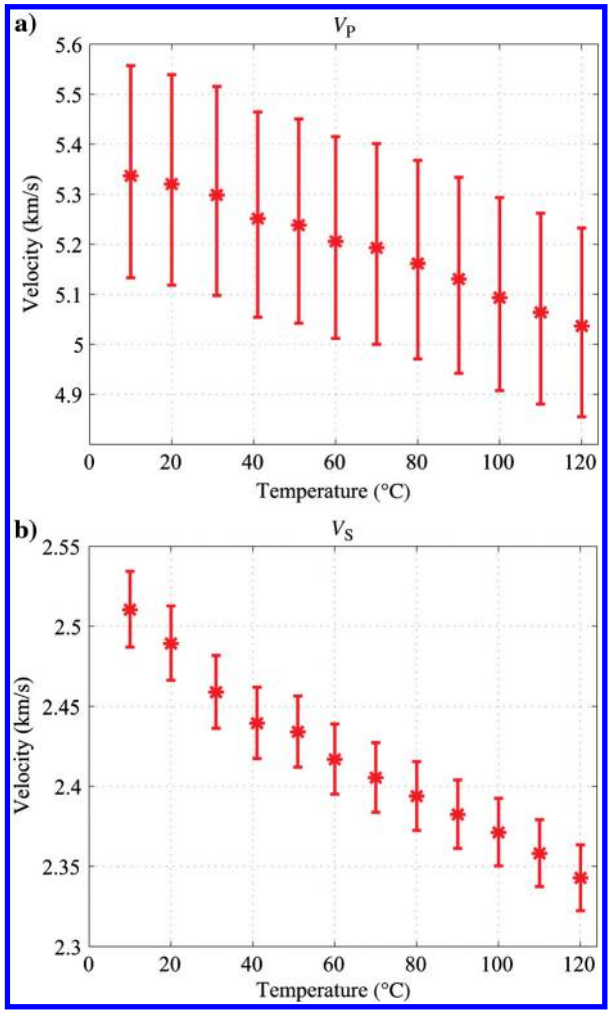

Figure 20. (a) The P-wave velocity and (b) S-wave velocity variations with temperature of cleaned sample 156A. Error bars are also plotted.

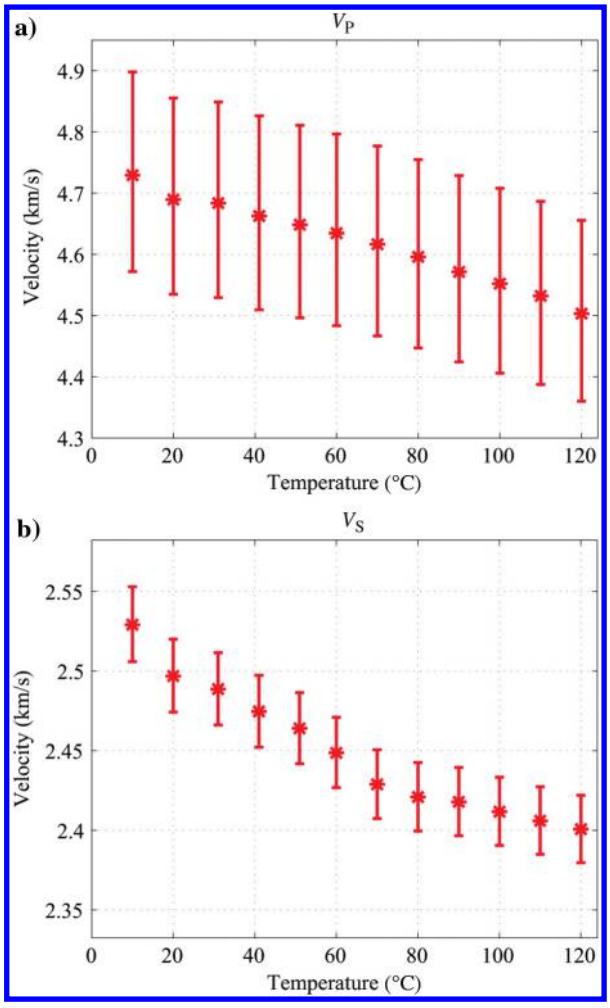

Figure 21. (a) The P-wave velocity and (b) S-wave velocity variations with temperature of cleaned sample 156B. Error bars are also plotted.

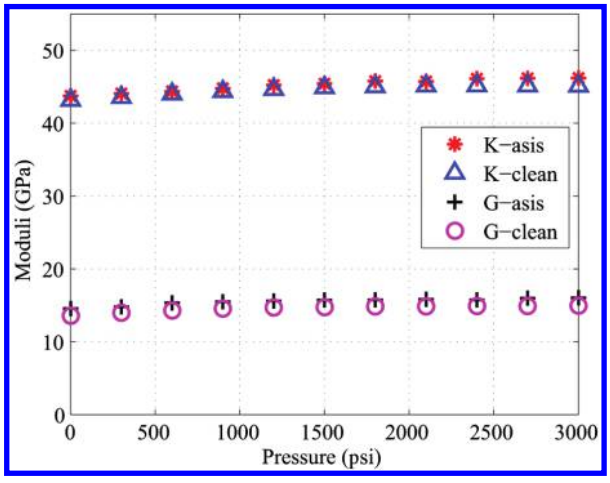

Figure 22. The moduli comparisons of the as-is sample and the clean sample of 156A under different pressures. The red asterisks represent the bulk modulus of the as-is sample, the blue triangles represent the bulk modulus of the clean sample, the black pluses represent the shear modulus of the as-is sample, and the magenta circles represent the shear modulus of the clean sample.

DISCUSSION

The porosity measurement method can estimate the porosity and bitumen saturation at the same time. It takes advantage of the property that bitumen appears as quasi-solid at room conditions. If the pore fluid is in liquid phase (e.g., water or oil), the method may fail to work, considering the possible fluid loss during the operation of the porosimeter.

Above measurements and analysis reveal that saturation of bitumen equips the carbonate samples with peculiar properties. In addition, the two samples show distinct trends at various pressure and

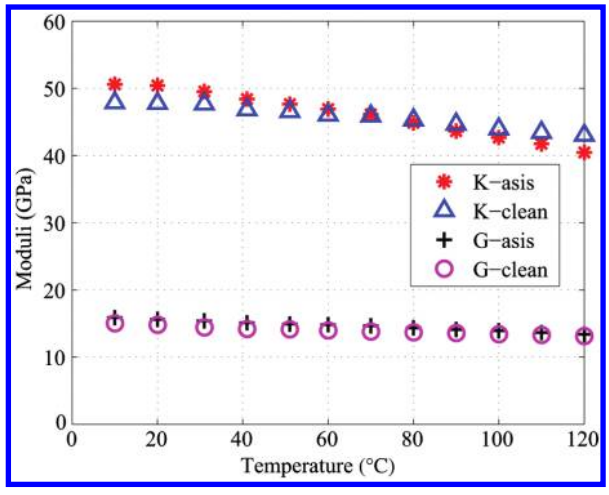

Figure 23. The moduli comparisons of the as-is sample and clean sample of 156A under different temperatures. The red asterisks represent the bulk modulus of the as-is sample, the blue triangles represent the bulk modulus of the clean sample, the black pluses represent the shear modulus of the as-is sample, and the magenta circles represent the shear modulus of the clean sample.

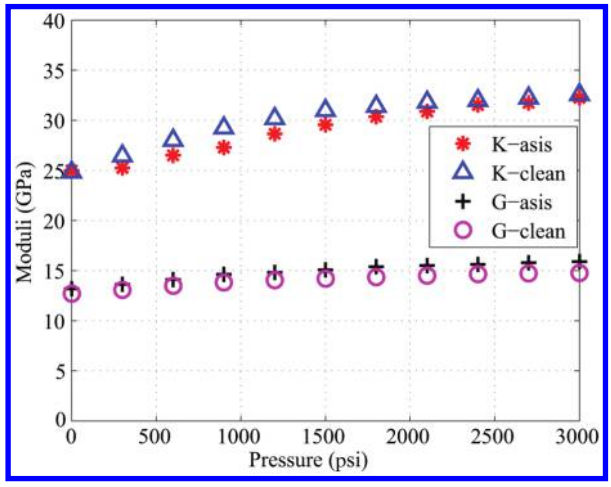

Figure 24. The moduli comparisons of the as-is sample and the clean sample of 156B under different pressures. The red asterisks represent the bulk modulus of the as-is sample, the blue triangles represent the bulk modulus of the clean sample, the black pluses represent the shear modulus of the as-is sample, and the magenta circles represent the shear modulus of the clean sample.

temperature conditions, which are probably related to porosity, bitumen saturation, and pore structure.

For the as-is sample, 156B appears to be more sensitive to pressure than 156A, as shown in Figure 25, which is attributed to its larger porosity and lower bitumen saturation. For pressures from 0 to 3000 psi, the V_P and V_S of 156B increase approximately 11% and 6.5%, whereas the V_P and V_S of 156A increase 3% and 5%, respectively, which is because the more empty pore space of 156B makes it more compressible. It is possible that the pore structure can also affect the samples' responses to pressure. In Figures 15a and 17a, the water saturation causes different P-wave velocities of the two samples. The V_P of wet 156A is smaller than the dry sample, which suggests that the pore structure is relatively stiffer so that the increase of bulk modulus due to water saturation is less than the increase of rock density; whereas the pore structure in 156B is relatively softer and the water saturation increases the bulk modulus more.

On the other side, 156A is more sensitive to temperature variations, as a result of its higher bitumen saturation. For temperatures from 10°C to 120°C, 156A has a 10% V_P drop and 8.4% V_S drop, whereas 156B has an 8% V_P drop and 8.2% V_S drop, indicating that 156A is more readily affected by the bitumen property. Different from bitumen sands that have large porosities and weak frame and thus can be easily damaged due to bitumen volume expansion during heating process (Han et al., 2007), bitumen carbonates in this case are well-consolidated with large frame moduli (Figures 22–25), suggesting that they are not easy to damage. Because the pores are not fully saturated and the carbonate samples are vacuumized before heating, the expanding bitumen would more readily fill the empty pore space rather than breaking the frame. Moreover, two measurements before and after the heating cycle (Figure 11) do not show noticeable changes, which also demonstrates that the frame of our carbonate samples is not severely affected by the bitumen expansion, and the velocity drop during heating is mainly caused by the variations of bitumen properties.

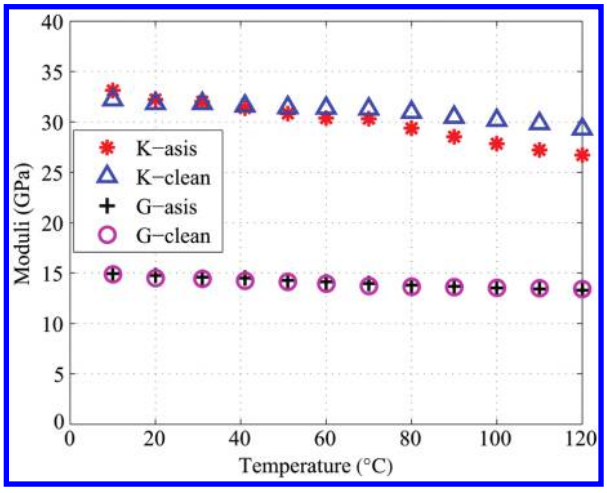

Figure 25. The moduli comparisons of the as-is sample and the clean sample of 156B under different temperatures. The red asterisks represent the bulk modulus of the as-is sample, the blue triangles represent the bulk modulus of the clean sample, the black pluses represent the shear modulus of the as-is sample, and the magenta circles represent the shear modulus of the clean sample.

In comparison with as-is samples, the clean samples show smaller V_P and V_S because the large bulk modulus and shear modulus of bitumen in the pore space make the as-is samples stiffer. The clean samples also display temperature-dependent behaviors, possibly related to the remaining bitumen in pore space. Regarding the temperature from 10°C to 120°C, the trends of bulk modulus of the as-is sample and clean sample cross each other, suggesting that the bitumen may have either a positive or a negative influence on carbonate modulus at different temperatures.

The dispersion effect between laboratory measurements at ultrasonic frequency and field seismic data is unavoidable, which is related to many factors, e.g., the bitumen itself and the rock frame heterogeneities. However, because the laboratory measurements are conducted at a unique frequency that is also the frequency of the transducer and the field seismic data are also in a certain frequency band, the dispersion would be nearly equal for all the measurements. Hence, we can bypass the dispersion effect through using relative velocity change, which might still be applicable for reservoir monitoring. For instance, the velocities drop more than 10% when the samples are heated at 120°C in the laboratory. And if the velocities of repeating survey show a decline more than 10%, then it can be concluded that the reservoir temperature is probably more than 120°C.

In this work, we have performed analysis of the properties of bitumen carbonates. However, there are still challenging problems before practical use. For instance, during thermal productions, the effects of pressure and temperature are coupled together. It is a challenge to predict the responses of the bitumen carbonates under various pressure and temperature conditions, which requires more comprehensive research on combining diverse factors.

CONCLUSION

We devise a method that can estimate the porosity and bitumen saturation simultaneously. The method can work well under the premise that the bitumen is in the solid state with the available density. Then, the elastic properties of bitumen carbonates are investigated by laboratory measurements.

To a great extent, the measurement conditions are similar to the field case. The measured pressures are the differential pressure and the range covers the in situ effective pressure. The measured temperatures, although lower than the field case, show significant influence on samples' velocities, which completely illustrates the influence of temperature.

Compared with the effect of pressure, the bitumen carbonate samples appear to be more sensitive to temperature. The V_P of 156A drops approximately 10% as temperature rises from 10°C to 120°C, whereas it drops less than 4% regarding pressure from 0 to 3000 psi. In addition, the velocities of the carbonate samples decline at larger rates when temperature is greater than 60°C, which may be related to the water-weakening effect because a high temperature softens the oil and makes it more displaceable by water.

After cleaning bitumen, the dry clean samples still show velocity variations at different temperature conditions, probably due to the remaining bitumen in the pore space. Besides, the bulk modulus of the as-is samples appears to be more susceptible to temperature change than the clean samples, as a result of the distinct phases of bitumen at different temperatures.

This study experimentally investigates the properties of bitumen-saturated carbonates under different pressure and temperature

conditions, and demonstrates that even under similar measurement conditions, different porosity, bitumen saturation, and pore structure can make the rocks behave distinctively. This is meaningful for us to improve the understanding of bitumen carbonates, and it is beneficial for industrial thermal production monitoring because it provides the potential responses of bitumen carbonates under different conditions.

ACKNOWLEDGMENTS

This work is supported by and the FLAG program is developed by Fluids and DHI consortium of Colorado School of Mines and University of Houston. The authors thank Cenovus Energy Inc. for providing the samples. The authors also thank the University of Copenhagen for support and their colleagues in Rock Physics Lab for discussion and advice.

REFERENCES

Adam, L., and M. Batzle, 2008, Elastic properties of carbonates from laboratory measurements at seismic and ultrasonic frequencies: The Leading Edge, **27**, 1026–1032, doi: 10.1190/1.2967556..

Adam, L., M. Batzle, and I. Brevik, 2006, Gassmann's fluid substitution and shear modulus variability in carbonates at laboratory seismic and ultrasonic frequencies: Geophysics, **71**, no. 6, F173–F183, doi: 10.1190/1.2358494.

Alboudwarej, H., J. Felix, S. Taylor, R. Badry, C. Bremmer, B. Brough, and C. Skeates, 2006, Highlighting heavy oil: Oilfield Review, **18**, 34–53.

Bakhorji, A. M., 2010, Laboratory measurements of static and dynamic elastic properties in carbonate: Ph.D. thesis, University of Alberta.

Batzle, M., R. Hofmann, and D. H. Han, 2006, Heavy oils — Seismic properties: The Leading Edge, **25**, 750–756, doi: 10.1190/1.2210074.

Carles, P., and P. Lapointe, 2004, Water-weakening of under stress carbonates: New insights on pore volume compressibility measurements: Presented at the International Symposium of the Society of Core Analysts held in Abu Dhab, SCA2004–27, 1–12.

Chen, X., A. Rabbani, D. Schmitt, and R. Kofman, 2015, Laboratory study of the seismic properties on bitumen saturated carbonates from Grosmont Formation, Alberta: 3rd International Workshop on Rock Physics, 1–3.

Dirgantara, F., M. Batzle, and J. Curtis, 2011, Maturity characterization and ultrasonic velocities of coals: 81st Annual International Meeting, SEG, Expanded Abstracts, 2308–2312.

Gassmann, F., 1951, Uber die elastizitat poroser medien: Veirteljahrsschrift der Naturforschenden Gesellschaft, **96**, 1–23.

Gomez, J. P., C. S. Rai, and C. H. Sondergeld, 2007, Effect of microstructure and pore fluid on the elastic properties of carbonates: 77th Annual International Meeting, SEG, Expanded Abstracts, 1565–1569.

Han, D. H., J. J. Liu, and M. Batzle, 2006, Acoustic property of heavy oil: 76th Annual International Meeting, SEG, Expanded Abstracts, 1903–1907.

Han, D. H., J. J. Liu, and M. Batzle, 2008, Seismic properties of heavy oils — Measured data: The Leading Edge, **27**, 1108–1115, doi: 10.1190/1.2978972.

Han, D. H., Q. Yao, and H. Zhao, 2007, Complex properties of heavy oil sans: 75th Annual International Meeting, SEG, Expanded Abstracts, 1609–1613.

Kato, A., 2010, Reservoir characterization and steam monitoring in heavy oil reservoirs: Ph.D. thesis, University of Houston.

Korsnes, R., M. Madland, T. Austad, S. Haver, and G. Rosland, 2008, Journal of Petroleum Science and Engineering, **60**, 183–193.

Kuila, U., 2013, Measurements and interpretation of porosity and pore size distribution in mudrocks: The hole story of shales: Ph.D. thesis, Colorado School of Mines.

Li, H., D. Han, H. Yuan, X. Qin, and L. Zhao, 2016a, Porosity of heavy oil sand: Laboratory measurement and bound analysis: Geophysics, **81**, no. 2, D83–D90, doi: 10.1190/geo2015-0178.1.

Li, H., L. Zhao, D. Han, M. Sun, and Y. Zhang, 2016b, Elastic properties of heavy oil sands: Effects of temperature, pressure, and microstructure: Geophysics, **81**, no. 4, D453–D464, doi: 10.1190/geo2015-0351.1.

Meyer, R., and E. Attanasi, 2003, Heavy oil and natural bitumen — Strategic petroleum resources: U.S. Geological Survey.

Priaro, M., 2014, Grosmont carbonate formation increases Alberta's bitumen reserves: Oil & Gas Journal, **7**, 58–64.

Rabbani, A., D. R. Schmitt, R. Kofman, and J. Nycz, 2014, Laboratory studies of the seismic properties of bitumen saturated Grosmont carbonates: AAPG Search and Discovery Article #90224.

Rabbani, A., D. Schmitt, J. Nycz, and K. Gray, 2017, Pressure and temperature dependence of acoustic wave speeds in bitumen-saturated carbonates: Implications for seismic monitoring of the Grosmont Formation: Geophysics, **82**, no. 5, MR133–MR151, doi: 10.1190/geo2016-0667.1.

Rojas, M. A., J. Castagna, R. Krishnamoorti, D. H. Han, and A. Tutuncu, 2008, Shear thinning behavior of heavy-oil samples: Laboratory measurements and modeling: 78th Annual International Meeting, SEG, Expanded Abstracts, 1710–1714.

Ruh, E. L., J. M. James, and R. D. Thompson, 1959, Measurement problems in the instrument and laboratory apparatus fields: American Association for Advancement of Science, **57**, 29.

Schmitt, D. R., 2002, Rock physics and time-lapse monitoring of heavy oil reservoirs: Presented at the SPE International Thermal Operations and Heavy Oil Symposium, 98075.

Schmitt, D. R., 2004, Oil sands and geophysics: CSEG Recorder, **29**, 5–11.

Scotellaro, C., and G. Mavko, 2008, Factors affecting the sensitivity of the elastic properties to pressure on carbonate rocks: 76th Annual International Meeting, SEG, Expanded Abstracts, 1665–1669.

Sharma, R., and M. Prasad, 2009, Characterization of heterogeneities in Carbonates: 79th Annual International Meeting, SEG, Expanded Abstracts, 2149–2154.

Wolf, K., 2010, Laboratory measurements and reservoir monitoring of bitumen-sand reservoir: Ph.D. thesis, Stanford University.

Yuan, H., D. Han, H. Li, and W. Zhang, 2017, A comparison of bitumen sands and bitumen carbonates: Measured data: Geophysics, **82**, no. 1, MR39–MR50, doi: 10.1190/geo2015-0657.1.

Yuan, H., D. Han, and W. Zhang, 2015, Heavy oil sands measurement and rock-physics modeling: Geophysics, **81**, no. 1, D57–D70, doi: 10.1190/geo2014-0573.1.